Oncogene (2011) 1–11

www.nature.com/onc

ORIGINAL ARTICLE

A novel tumor-derived SGOL1 variant causes abnormal mitosis and unstable chromatid cohesion

T Kahyo[1], M Iwaizumi[1,2], K Shinmura[1], S Matsuura[1,3], T Nakamura[4], Y Watanabe[5], H Yamada[1] and H Sugimura[1]

[1]First Department of Pathology, Hamamatsu University School of Medicine, Hamamatsu, Japan; [2]First Department of Medicine, Hamamatsu University School of Medicine, Hamamatsu, Japan; [3]Second Department of Medicine, Hamamatsu University School of Medicine, Hamamatsu, Japan; [4]Second Department of Surgery, Hamamatsu University School of Medicine, Hamamatsu, Japan and [5]Laboratory of Chromosome Dynamics, Institute of Molecular and Cellular Biosciences, University of Tokyo, Tokyo, Japan

Mitosis is the most conspicuous cell cycle phase, because it is the phase in which the dynamic physical distributions of cellular components into the two daughter cells occur. The separation of sister chromatids is especially important during mitosis, because of the extreme accuracy required for distribution to the next generation of cells. Shugoshin-like 1 (SGOL1) is a key protein in protecting sister chromatids from precocious separation. We have reported finding that chromosome instability is more likely in SGOL1-downregulated colorectal cancers, but it is still unknown whether there is an association between cancer and SGOL1 transcript variation. Here, we identified a novel SGOL1 variant, SGOL1-P1, in human colon cancer. The SGOL1-P1 transcript contains an exon-skip of exon 3 that results in a stop codon occurring within exon 4. Overexpression of SGOL1-P1 in HCT116 cells resulted in an increased number of cells with aberrant chromosome alignment, precociously separated chromatids and delayed mitotic progression, occasionally followed by inaccurate distribution of the chromosomes. These phenotypes, observed when SGOL1-P1 was present, were also observed very frequently in SGOL1-knockdown cells. Furthermore, the overexpression of SGOL1-P1 inhibited the localization of endogenous SGOL1 and cohesin subunit RAD21/SCC1 to the centromere. These results suggest that SGOL1-P1 may function as a negative factor to native SGOL1, and that abundant expression of SGOL1-P1 may be responsible for chromosomal instability.
Oncogene advance online publication, 2 May 2011; doi:10.1038/onc.2011.152

Keywords: chromosomal instability; colon cancer; mitosis; shugoshin; splicing variant

Correspondence: Dr H Sugimura, First Department of Pathology, Hamamatsu University School of Medicine, 1-20-1 Handayama, Higashi-ku, Hamamatsu, Shizuoka 431-3192, Japan.
E-mail: hsugimur@hama-med.ac.jp
Received 3 October 2010; revised and accepted 26 March 2011

Introduction

Accurate separation of sister chromatids to opposite poles during mitosis is necessary to ensure euploidy in the daughter cells, because once the sister chromosomes have incorrectly separated, they cannot revert to their original distribution in the normal nucleus. Aberrant distribution of chromosomes into daughter cells induces chromosomal instability (CIN) and often leads to aneuploidy (Rajagopalan and Lengauer, 2004). CIN frequently occurs in human malignant tumors (Lengauer *et al.*, 1998) and it is a major cause of genomic instability in colorectal cancer (Grady, 2004). Two causes of CIN have been reported: a defect in the spindle assembly checkpoint (SAC) and a defect in centrosome replication, both of which can be induced by a mutation in a checkpoint gene or by an exogenous agent (Pihan and Doxsey, 1999; Shinmura *et al.*, 2008). As chromosomes are exposed to the greatest risk of CIN during mitosis, analysis of mitotic progression has become a focus of attention in the field of cancer research (Bharadwaj and Yu, 2004).

The function of the cohesin complex is to physically bind sister chromatids from the genomic replication phase of the cell cycle until segregation at anaphase (Nasmyth *et al.*, 2000). Although the bulk of cohesin is removed during prophase and prometaphase, centromere cohesin persists throughout metaphase (Waizenegger *et al.*, 2000) and is finally cleaved by separase during anaphase (Hauf *et al.*, 2001). Kinetochore fiber microtubules from bipolar spindle poles attach to sister chromatids at the kinetochore. When spindle microtubules fail to attach to the kinetochore, SAC instead functions to prevent premature chromatid segregation. The premature segregation is prevented by the recruitment of SAC proteins to unattached kinetochores, which inhibits the cleavage of cohesin complex through the signaling cascade (Peters, 2002).

Originally, shugoshin/MEI-S332 (Sgo1) was identified in *Drosophila* as a mutant, defective in sister chromatid cohesion in meiosis (Goldstein, 1980) and reported to enrich at the centromere until sister chromatids separate (Kerrebrock *et al.*, 1995; Moore *et al.*, 1998). Further studies revealed that Sgo1 is a protector of

Rec8, a component of meiotic cohesin, in yeast (Kitajima *et al.*, 2004; Marston *et al.*, 2004; Rabitsch *et al.*, 2004; Clift *et al.*, 2009) and that it is essential for accurate sister chromatid separation during mitosis in vertebrates (Salic *et al.*, 2004; Tang *et al.*, 2004; Kitajima *et al.*, 2005; McGuinness *et al.*, 2005). Shugoshin-like (SGOL1) protein, the mammalian homolog of shugoshin, interacts with protein phosphatase 2A (PP2A), localizes in the centromeric region and prevents cohesin complex from precocious cleavage at the centromere through dephosphorylation of SA2, one of the cohesin subunits (Kitajima *et al.*, 2006; Riedel *et al.*, 2006). In a study on human cancer, we found that SGOL1 expression was decreased in colorectal cancer and that SGOL1-knockdown led to CIN in a colon cancer cell line (Iwaizumi *et al.*, 2009). Furthermore, a crucial link between histone H2A phosphorylation and CIN through shugoshin has recently been discovered (Kawashima *et al.*, 2010). These reports on shugoshin and SGOL1 indicate that shugoshin is a cross-species guardian at the centromere.

Many tumor-specific splicing products have been studied in a variety of tumors. Although a variant-generating model in cancer has been suggested (Mayr and Bartel, 2009), no common theory applicable in all cancers has ever been proposed. In addition to the major splicing variants A1 and A2, 527 and 561 amino acids, respectively, some short variants of SGOL1 have been analyzed, and it has been suggested that the short variants have a negative effect on the cohesion between sister chromatids (Suzuki *et al.*, 2006). However, no association between disease and *SGOL1* transcript variants has ever been shown.

In this paper, we report a novel *SGOL1* variant that was detected preferentially in tumor tissue. Forced expression of the tumor-associated variant resulted in abnormal mitotic progression and premature separation between sister chromatids in a colon cancer cell line, as same as in SGOL1-knockdown cells, suggesting that the tumor-associated variant interferes with native SGOL1 and can serve as a target for treatment.

Results

SGOL1-P1 expressed in colon cancer

A variety of *SGOL1* variants have been registered in the NCBI protein database (Figure 1a). To investigate whether there is an association between colon cancer and a particular *SGOL1* transcript variant, a reverse transcription-polymerase chain reaction (RT–PCR) was performed with total RNA from specimens of human colon cancer (Figure 1b). Many types of amplified products were detected from tumor tissue, but only one or two variants were amplified from normal tissue, and several products were cloned and sequenced from tumor tissue. A novel *SGOL1* variant named *SGOL1-P1* was identified among the sequenced clones derived from the tumor tissue. The sequence data of *SGOL1-P1* have been submitted to the DDBJ (DNA Data Bank of Japan) database under accession numbers AB567656 and AB567657. The *SGOL1-P1* transcript lacks the exon 3 region and has a frameshift that causes a premature stop codon to occur within exon 4 (Supplementary Figure S1). PCR analysis using the primer specific for *SGOL1-P1* showed that the prevalence of *SGOL1-P1* expression was 6/46 (13.0%) in colon tumors and that no *SGOL1-P1* was expressed in the adjacent non-tumor tissue (Figure 1c). Total expression of other variants, except P1, was lower in the tumor tissue expressing *SGOL1-P1* than in paired non-tumor tissues (Figure 1d), indicating that the emergence of *SGOL1-P1* was not caused by acceleration of *SGOL1* gene expression. In addition, we isolated 1.75-fold more SGOL1-P1 clones, by a series of procedures including RT–PCR, TA-cloning, and picking and counting the colonies, than the SGOL1-A variants clones from tumors. This result excludes the possibility that the P1 is a rare and artificial transcript in human tumors; instead, it suggests that P1 variant affects the wild type SGOL1 as a dominant negative form in the clinical setting. SGOL1-P1 is composed of 59 amino acids, including the short coiled-coil region determined by the *Coils2* program (Lupas *et al.*, 1991) (Figure 1e). This region is well conserved among vertebrates (Supplementary Figure S2). Interestingly, the *SGOL1-P1*-positive tumors were smaller than the *SGOL1-P1*-negative tumors (Figure 1f). None of the *SGOL1-P1*-positive tumors was larger than the average of the tumors as a whole. These results show that *SGOL1-P1* is preferentially expressed in colon cancer and that there is a correlation between *SGOL1-P1* expression and tumor size.

Aberrant chromosome alignment during mitosis in cells expressing SGOL1-P1

To investigate the effect of SGOL1-P1 on cell division, we overexpressed SGOL1-P1 in HCT116 cells, human colorectal cancer cells, and observed the mitotic cells. Interestingly, the chromosome mass in the SGOL1-P1-transfected cells appeared spread out and not to be precisely aligned with the metaphase plate (Figure 2a). According to previous papers, aberrant chromosome alignment was observed in SGOL1-knockdown cells (Salic *et al.*, 2004; Tang *et al.*, 2004; Kitajima *et al.*, 2005, 2006). We therefore analyzed chromosome alignment at prometaphase and metaphase in detail in the present study in order to investigate the function of SGOL1-P1. For this analysis, chromosome alignment index was calculated on the basis of the shape of chromosomal mass (Figures 2a and b). The results of the morphometric analysis of the images acquired in the present study showed that the frequency distributions of the chromosome alignment index values of SGOL1-knockdown cells (SGOL1 RNAi) and SGOL1-P1-overexpressing cells were lower than those of the control cells (control RNAi) and the cells transfected with empty vector, respectively (Figures 2c–f). These results indicate that SGOL1-P1 overexpression leads to aberrant chromosome alignment, the same way as SGOL1-knockdown does. When the chromosomal mass is not positioned parallel to the horizontal plane, the

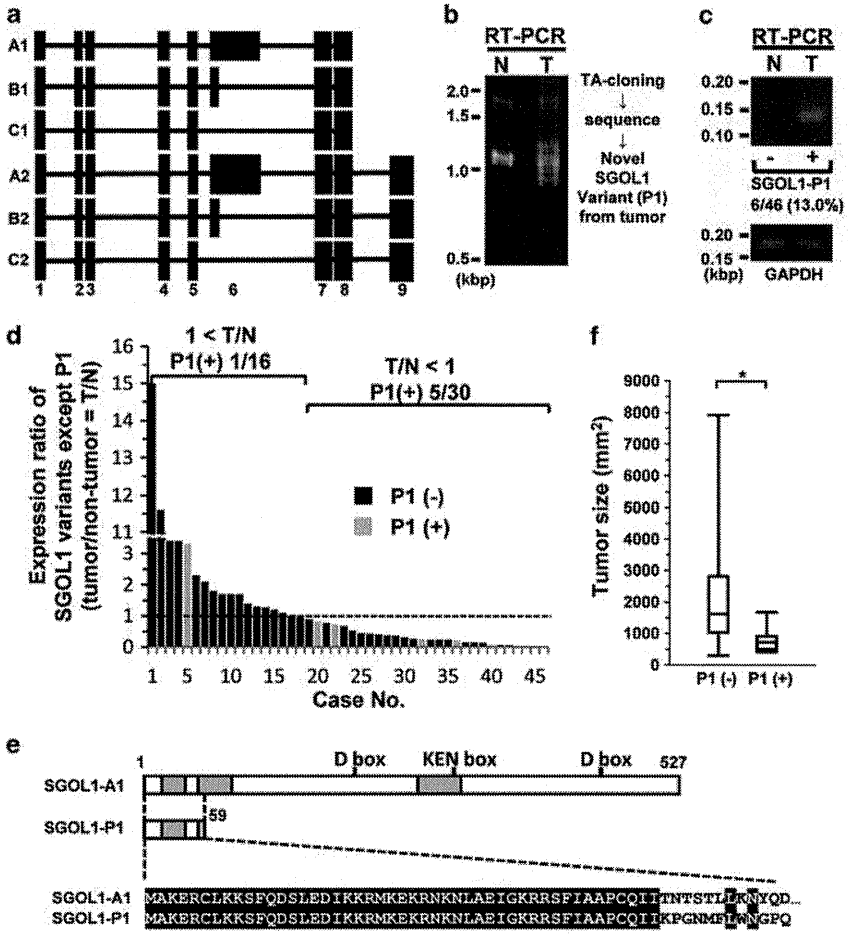

Figure 1 A novel SGOL1 variant expressed in colon cancer. (**a**) Scheme of SGOL1 transcript variants. Filled boxes represent exon regions (exons 1–9). (**b**, **c**) Total RNAs from colon cancer specimens were used to perform RT–PCR. Some products were amplified with the primers targeting exon 1 and exon 8 (**b**). Primers targeting the exon 2–4 junction and exon 5 of SGOL1 were also used (**c**). GAPDH was amplified as an internal control. N = non-tumor, T = tumor. (**d**) Quantitative real-time RT–PCR analysis of *SGOL1* variants, except P1. The primers targeting exon 3 and exon 4 of *SGOL1* were used. They are applicable for amplification of exon 3-containing *SGOL1* transcripts. (**e**) Amino acid alignment of SGOL1-A1 and SGOL1-P1. The gray areas indicate the coiled-coil regions. Both of D box and KEN box are known as motifs for destruction. The white letters on the black background represent amino acids that are identical in both variants. (**f**) Correlation between the presence of *SGOL1-P1* transcripts and tumor size. Tumor size was calculated by multiplying the length of the major axis by the length of the minor axis. P1(−), $n=40$; P1(+), $n=6$. $^*P<0.05$ (Mann–Whitney *U*-test).

calculated index value may not be appropriate for estimating the deviation of the chromosomes from the metaphasic plate. However, the distributions of the angles of the spindle bodies relative to the horizontal plane were similar among the various groups of cells that were examined (Supplementary Figure S3). Thus, the angle of the chromosomal mass relative to the horizontal plane may not have influenced the calculated index values in the present study.

Delayed mitotic progression in cells expressing SGOL1-P1

As the aberrant alignment in Figure 2a resembled the mitotic progression defect observed in SGOL1-knockdown cells reported previously (Salic *et al.*, 2004; McGuinness *et al.*, 2005), we performed time-lapse imaging to investigate the aberrant chromosome alignment, and we used GFP-histone H2B to observe the chromosome dynamics in living cells (Kanda *et al.*, 1998). Measurements of the time taken to progress from prophase to anaphase revealed severe mitotic arrest in SGOL1-knockdown cells (Figure 3a). It took 50 min or more for 50% of the cells (52/105) to move from prophase to anaphase. Most of the cells exhibiting this delayed phenotype (34/52, 65.4%) had not reached anaphase within the observation period, because prometaphase or metaphase had lasted several hours or more. The cells transfected with SGOL1-P1 also showed a progression delay compared with the cells transfected with SGOL1-A1 and the cells transfected with the empty control vector (Figure 3b). The subfraction of cells whose progression time between prophase and anaphase was 50 min or more was larger among the cells

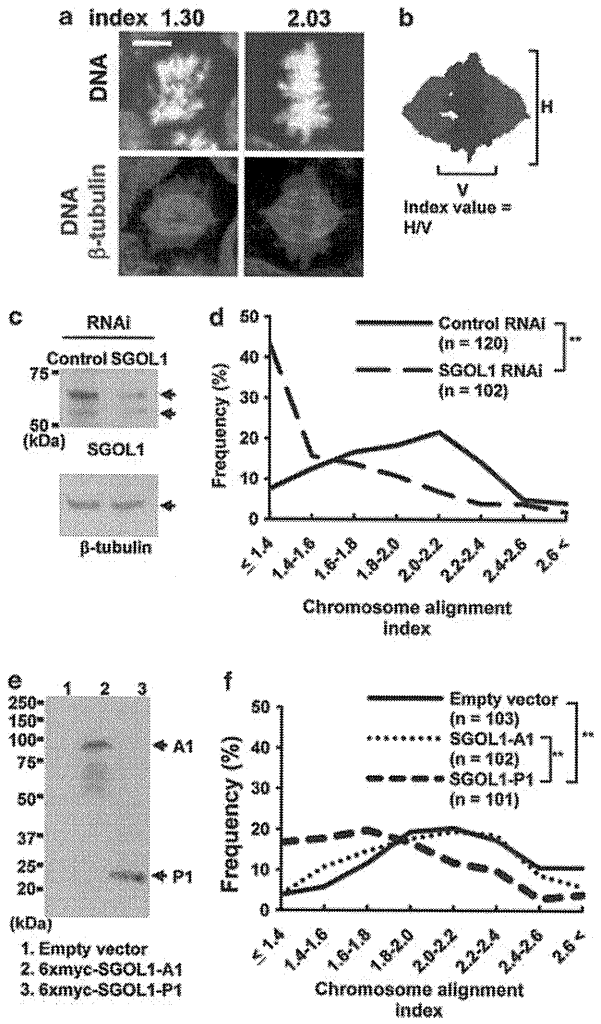

Figure 2 Aberrant chromosome alignment in mitotic cells expressing SGOL1-P1. (**a**) HCT116 cells were transfected with pSilencer-SGOL1 and myc-SGOL1 (A1 and P1) for knockdown and overexpression, respectively. Following antibiotic selection, the cells were subjected to immunofluorescence staining with anti-β-tubulin antibody and DAPI, and Z-stacked confocal images were acquired. Representative fluorescence images of the mitotic cells transfected with myc-SGOL1-P1 (left) and myc-SGOL1-A1 (right) are shown. Scale bar = 5 μm. (**b**) The chromosome alignment index was calculated as H/V, in which H and V are the horizontal length and vertical length, respectively, of the chromosomal mass at the metaphase plate. The blue area and the red areas represent the chromosomal mass and the spindle body, respectively. (**c**, **e**) Immunoblotting with rabbit anti-shugoshin antibody (**c**) and anti-myc antibody (**e**) was performed to confirm the effect of transfection. The graphs indicate frequency distribution of the ranges of chromosome alignment index values (**d**, **f**). $^{**}P<0.01$ (χ^2-test).

transfected with SGOL1-P1 (8/102, 7.84%) than among the cells transfected with SGOL1-A1 (3/125, 2.40%) or the cells transfected with the empty control vector (2/116, 1.72%). The chromosomes of the cells that exhibited delayed progression seemed to fumble for the metaphase plate (Figures 3c and d, and Supplementary Movie 1). The chromosomal masses in some SGOL1-P1 transfected cells (3/102, 2.94%) separated without congressing at the metaphase plate, but no such cells were observed among the cells transfected with SGOL1-A1 or the empty control vector (Figure 3e and Supplementary Movie 2). These results show that SGOL1-P1 expression prevents mitotic progression to anaphase and causes inaccurate chromosome distribution.

Decrease in centromeric localization of endogenous SGOL1 in cells expressing SGOL1-P1

Overexpressed SGOL1-P1 was localized in both the cytoplasm and the nucleus at interphase and outside the chromosomes during mitosis (Figure 4a). Furthermore, SGOL1-P1 was abundantly present even at anaphase (Figure 4a and Supplementary Figure S4a), whereas endogenous SGOL1 was not observed as described previously (Salic *et al.*, 2004). SGOL1-P1 lacks the motifs for destruction that are present in the long form of SGOL1 (Figure 1e; Karamysheva *et al.*, 2009). Therefore, the result that SGOL1-P1 was abundantly present at anaphase is consistent with its amino acid sequence. In some cases, abnormal segregations of chromosomes, such as that shown in Figure 3e, were observed in the SGOL1-P1-expressing cells (Figure 4a). The cyclin B1 level in cells exhibiting abnormal chromosome segregation was higher than that in cells exhibiting typical anaphase and similar to the level observed in metaphase cells (Supplementary Figure S4b). The anaphase-promoting complex/cyclosome (APC/C), which is a ubiquitin-ligase and targets cell-cycle-related proteins (including cyclin B1) for degradation by the 26S proteasome and promotes exit from metaphase, is suppressed during SAC activation (Wasch *et al.*, 2010). Therefore, our results show that abnormal chromosome segregation did not follow the degradation of cyclin B1, suggesting that SAC remains activated in cells in which abnormal chromosome segregation occurs. To investigate the effect of SGOL1-P1 on endogenous SGOL1 at mitosis, we performed a co-immunofluorescence study for the centromere, endogenous SGOL1 and myc-SGOL1-P1. Interestingly, we found that the endogenous SGOL1 signals at the centromere decreased in the SGOL1-P1-expressing cells (Figure 4b), where the metaphasic chromosomes had a defective alignment as shown in Figure 2. Because SGOL1 prevents cohesin from precocious cleavage at the centromere, we investigated whether RAD21/SCC1, a cohesin subunit, was localized at the centromere. The signals of RAD21 at the centromere also decreased in the SGOL1-P1-expressing cells with the alignment defect (Figure 4c), whereas the signals of PP2A-B56α, a regulatory subunit of the PP2A complex, did not (Figure 4d). These results show that SGOL1-P1 inhibits the localization of native SGOL1 and RAD21 to the centromere, independently of PP2A.

Cohesion defects between sister chromatids in cells expressing SGOL1-P1

The result that RAD21 decreased at the centromere in SGOL1-P1-expressing cells reminded us that cohesion

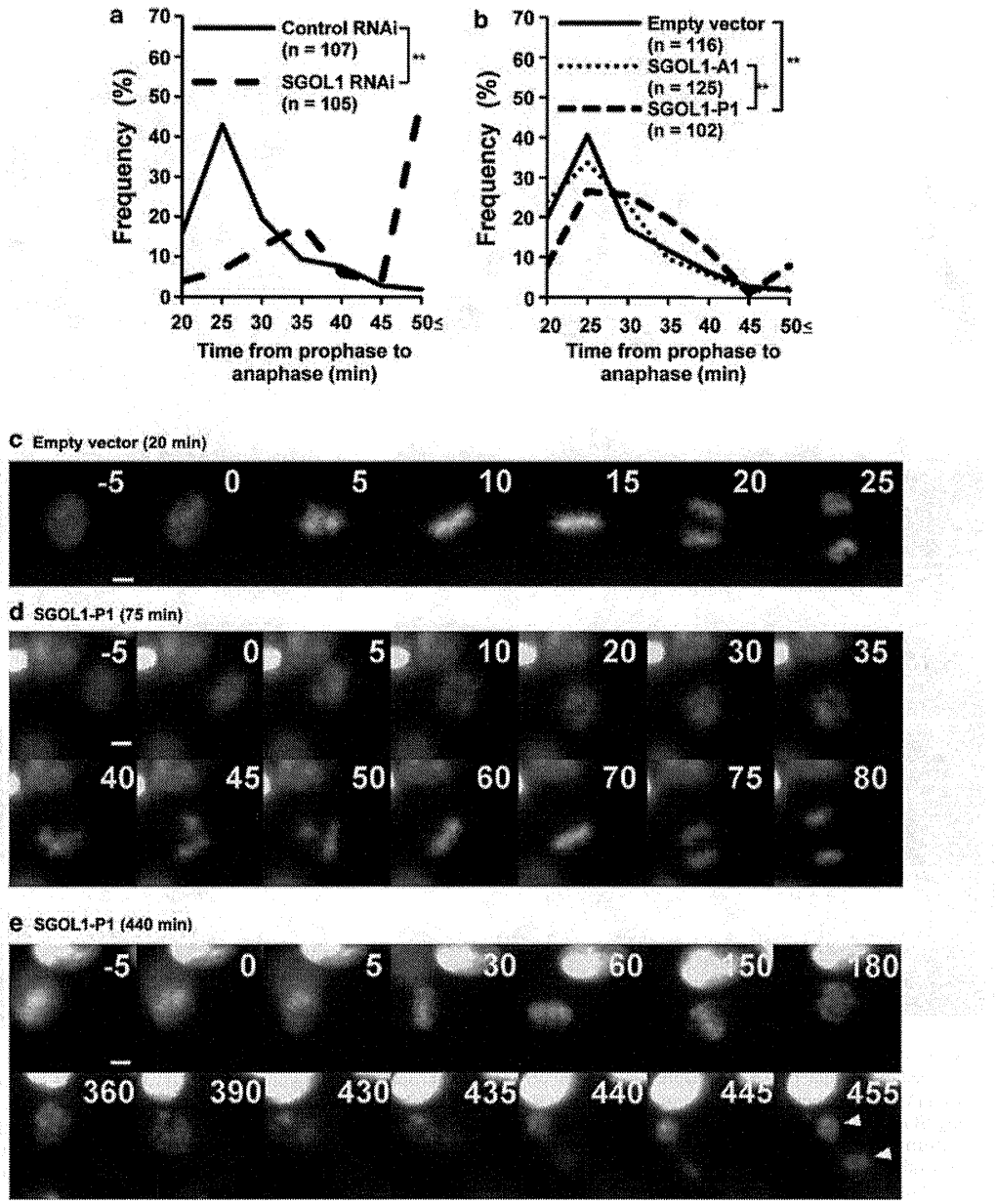

Figure 3 Delayed mitotic progression in cells expressing SGOL1-P1. (**a**, **b**) GFP-histone H2B was co-transfected with pSilencer-SGOL1 or myc-SGOL1, and time-lapse images of the cells were taken at 5 min intervals. The graphs indicate frequency of progression times from nuclear envelope breakdown or chromatin condensation (prophase) to the onset of chromosome-to-pole movement (anaphase). Total cell counts are shown in the graphs. (**c**–**e**) Representative montage images of normal mitotic progression (**c**), delayed progression (**d**, **e**) and abnormal chromosome segregation with immature congression at the metaphase plate (**e**). Arrowheads indicate daughter nuclei. Time in minutes is shown at the upper right of each panel. Scale bar = 5 μm. $^{**}P<0.01$ (χ^2-test).

defect between sister chromatids occurred. To assess the effect of SGOL1-P1 on sister chromatid cohesion, a chromosome spread assay was performed. Spread chromosomes were stained with DAPI (Figure 5a) and the frequency of the each of the separation patterns was counted (Figure 5b). The SGOL1-knockdown cells exhibited a high frequency of severe cohesion defects between sister chromatids, the same as described previously (Tang *et al.*, 2004; Kitajima *et al.*, 2005; McGuinness *et al.*, 2005). Severe cohesion defects were also observed in 11% of the SGOL1-P1-expressing cells, but they were rarely found in the control cells. Cells defecting cohesion between sister chromatids are prone to develop CIN as a result of failure of mitotic progression. Because HCT116 cells have a relatively stable karyotype (45 chromosomes; Kienitz *et al.*, 2005), the total number of chromosomes per cluster can be counted. The frequency of the aberrant phenotype, which we defined as a cluster composed of more than 50 chromosomes, was significantly higher in the

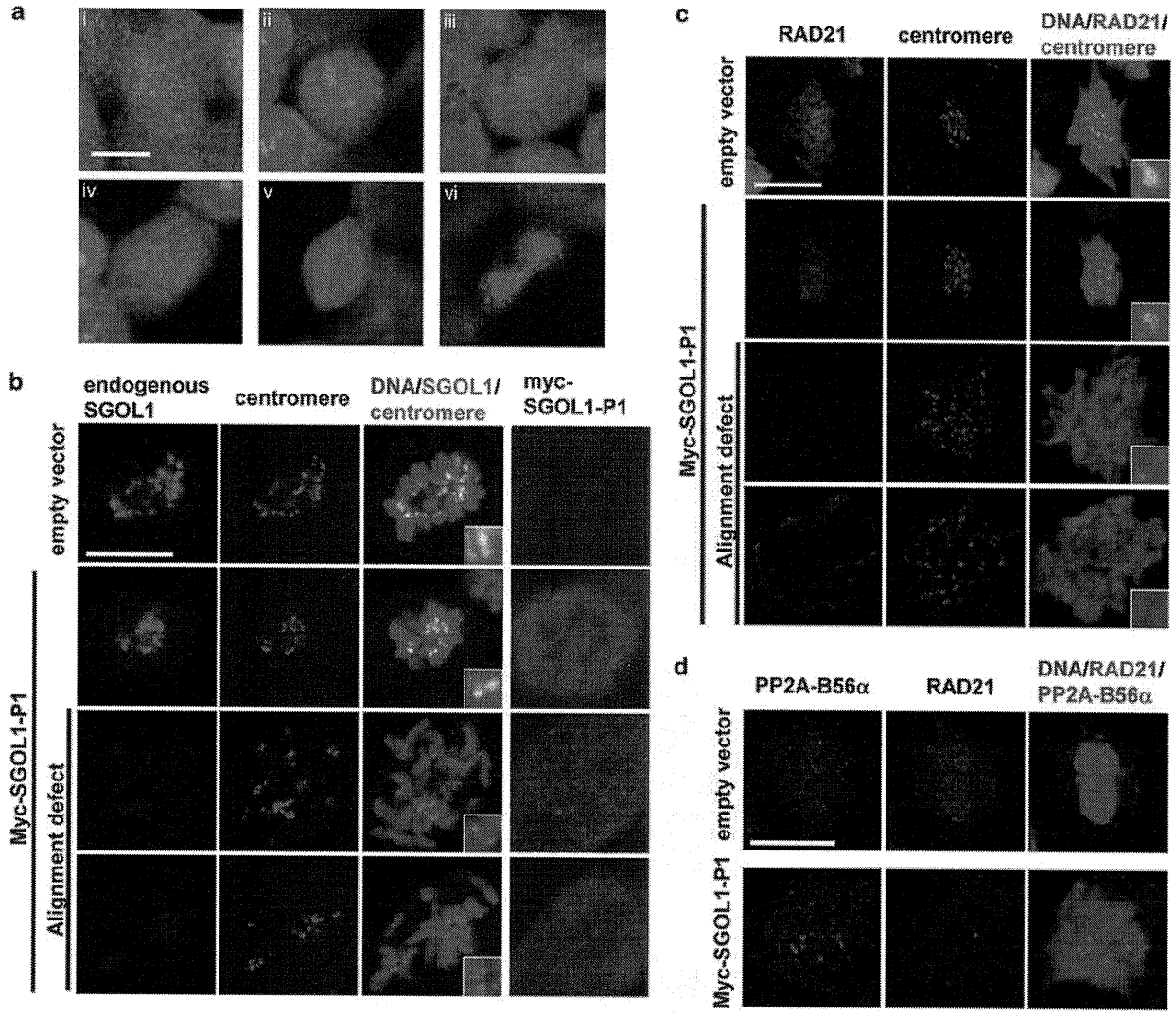

Figure 4 Decrease in centromeric localization of endogenous SGOL1 in cells expressing SGOL1-P1. (**a**) Localization of SGOL1-P1 during the cell cycle. Interphase (I), prophase (II), metaphase (III), chromosomal alignment defect (IV), anaphase (V) and abnormal segregation (VI) are shown with the staining of myc-SGOL1-P1 (red) and DNA (blue). (**b**) Localization of endogenous SGOL1 in cells expressing SGOL1-P1. HCT116 cells were transfected with myc-SGOL1-P1. Following culture with an antibiotic, the cells were fixed with paraformaldehyde (**a**, **b**). Endogenous SGOL1 and myc-SGOL1-P1 were detected using immunofluorescence with mouse anti-hSgo1 and rabbit anti-myc antibodies, respectively. (**c**, **d**) Localization of endogenous RAD21 and PP2A-B56α on chromosomes in cells expressing SGOL1-P1. For the immunostaining of RAD21 and PP2A-B56α, the cells were fixed with paraformaldehyde, followed by spinning down on a glass coverslip and pre-extraction with a detergent. The centromere was detected using immunofluorescence with human anti-centromere autoantibody (**b**, **c**). The inset is a magnified image of the centromere. Scale bar = 10 μm.

SGOL1-knockdown cells ($P = 0.037$, Fisher's exact test), and the frequency of the phenotype tended to be higher in the SGOL1-P1-expressing cells than in the control cells ($P = 0.097$) (Figures 5c and d). These results mean that SGOL1-P1 participates in the precocious separation of sister chromatids and is capable of inducing CIN in the process of cell proliferation.

Abnormal cell phenotypes in the stable cell lines expressing SGOL1-P1

To examine the effects of SGOL1-P1 expression during long-term culture, we established cell lines stably expressing SGOL1-P1 (P3-2 and P4-1) from HCT116 cells (Figure 6a). These cell lines exhibited a slightly higher mitotic frequency, particularly in prometaphase/metaphase, than the parental cell and the stable cell line transfected with the empty vector (Table 1 and Figure 6b). They were also observed to exhibit delayed mitotic progression (Supplementary Figure S5a) and chromosome separation without congression at the metaphase plate when examined by time-lapse fluorescence microscopy (Table 1, Supplementary Figure S5b and Supplementary Movies 3 and 4). The delayed mitotic progression is consistent with the mitotic frequency data. The time-lapse data also indicated that P3-2 and P4-1 have the same properties during mitosis as cells that transiently express SGOL1-P1.

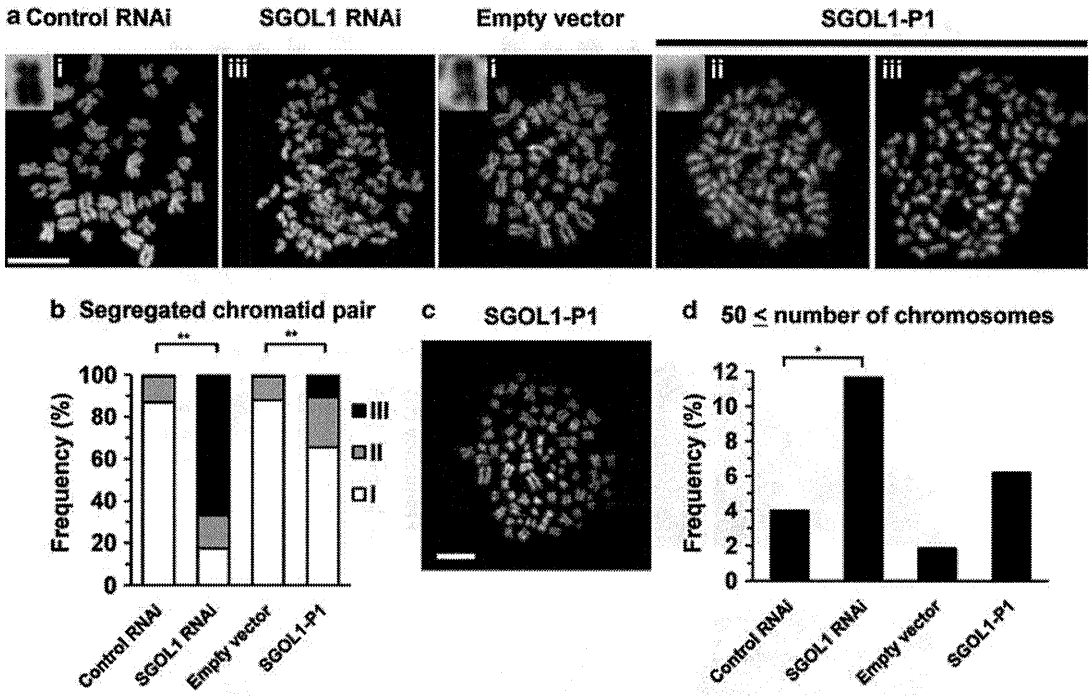

Figure 5 Cohesion defects between sister chromatids in cells expressing SGOL1-P1. (**a**) Representative images of chromosome spread. Transfected HCT116 cells were treated with 100 nM nocodazole for 18 h to arrest the cell cycle during mitosis. Spread chromosomes stained with DAPI were classified into the following three patterns: (I) normal cohesive chromatids or only a very few pairs of separated sister chromatids; (II) separated chromatids have remained in close proximity to the pair partner (several chromatid pairs remain cohesive); and (III) severely separated chromatids (the pair partner is often hard to identify, because it is located some distance away). A representative image of the chromatid pairs exhibiting patterns I and II is inverted and magnified in the left top panel. (**b**) Frequency of cells with cohesion defects between sister chromatids. (**c**) A representative image of a phenotype with an increased number of chromosomes (78 chromosomes). (**d**) The graph shows the frequency of 50 or more chromosomes. Total cell number: Control RNAi, 100; SGOL1 RNAi, 103; empty vector, 108; SGOL1-P1, 113. Scale bar = 10 μm. $^{*}P<0.05$ (Fisher's exact test), $^{**}P<0.01$ (χ^2-test).

Abnormal nuclear shape is known to reflect CIN and to be frequently observed in malignant tumors (Gisselsson *et al.*, 2001). The stable cell lines expressing SGOL1-P1 exhibited less circularity and more frequent micronuclei (Table 1 and Figures 6c and d). We examined cells for the presence of an extra centrosome, because multiple spindle poles have been reported to be common in mitotic SGOL1-knockdown cells (Kitajima *et al.*, 2006; Dai *et al.*, 2009). An extra centrosome was observed more frequently in the cell lines expressing SGOL1-P1 (Table 1 and Figure 6e). Triple daughter nuclei, caused by multiple spindle formation, were also observed almost exclusively in cells expressing SGOL1-P1 (Supplementary Figure S5c and Supplementary Movie 5). We suspected that the culture time of several days shown in Figure 5d was not long enough to induce a full-blown aberrant phenotype in the SGOL1-P1-expressing cells. The increased number of chromosomes mentioned here reflects the aberrant distribution of chromosomes preceding mitosis. Thus, a shorter culture time may not yield sufficient chromosome aberrations from the previous mitosis. Therefore, we examined the number of chromosomes in SGOL1-P1-stably expressing cells, which had passed through more mitotic phases. In addition to the premature separation of sister chromatids, an aberrant number of chromosomes was observed more frequently in cells expressing SGOL1-P1 than in the parent cells (Figures 6f and g). These results indicate that long-term expression of SGOL1-P1 affects nuclear shape, centrosome stability and CIN.

Discussion

SGOL1-P1 was identified as a novel tumor-specific variant and the *SGOL1-P1*-positive tumors were smaller than the *SGOL1-P1*-negative tumors. Because the outcome of the *SGOL1-P1*-positive cases is still unknown, the relationship between *SGOL1-P1* expression and the prognosis remains unclear. As our observations in this study showed that SGOL1-P1 expression induced the HCT116 aberrant karyotype, abnormal nuclear shapes and micronuclei, all of which are indicative of the highly malignant nature of the tumor cells, SGOL1-P1 may drive early stage tumors toward a more aggressive phenotype. After SGOL1-P1 has driven a small benign tumor to undergo malignant transformation, it may not be required for tumor progression. *SGOL1-P1* would rarely be observed in an advanced tumor. This model, in which SGOL1-P1 causes malignancy in the early stage of colon cancer, may be applicable to other types of cancer because *SGOL1-P1* was also detected in lung cancer (Supplementary Figure S6). Comprehensive analysis of the role of SGOL1-P1 is now under way in lung cancer.

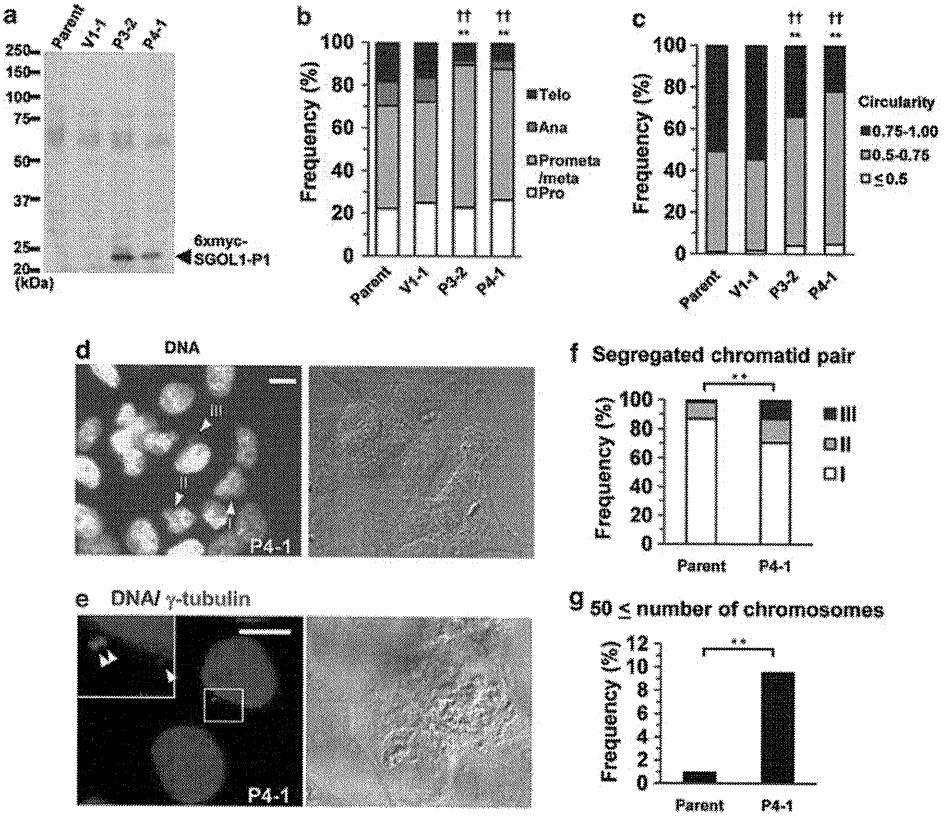

Figure 6 Aberrant cell phenotypes and mitotic progression in cells constitutively expressing SGOL1-P1. (**a**) Stable cell lines were produced from HCT116 cells. P3-2 and P4-1 are the cell lines expressing myc-SGOL1-P1, whereas V1-1 is a cell line derived from the cells transfected with empty vector. Anti-myc antibody was used for the immunoblotting. (**b–d**) The stable cell lines and parental cells were stained with DAPI. The graph shows the frequency of each mitotic phase (**b**). Nuclear circularity was calculated by using the formula: $4\pi \times A/p^2$ (A = area, p = perimeter) (**c**). Representative distorted nuclei (arrowheads 'I' and 'II') and a micronucleus ('III') are shown (**d**). (**e**) Immunofluorescence staining was performed with anti-γ-tubulin antibody. A magnified image is shown in the left top panel. Arrowheads indicate centrosomes. The panel on the right is a merged image of DNA (blue) and differential interference contrast (gray). (**f, g**) Chromosome spread assay was performed with P4-1 and parent cells as described in Figure 5. Total cell numbers: Parent, 1027 (**b**), 418 (**c**) and 106 (**f, g**); V1-1, 1130 (**b**) and 441 (**c**); P3-2, 1106 (**b**) and 452 (**c**); P4-1, 1152 (**b**), 403 (**c**) and 105 (**f, g**). Scale bar = 10 μm. $^{**}P<0.01$ vs parent, $^{\dagger\dagger}P<0.01$ vs V1-1 (χ^2-test). Fisher's exact test was also used (**g**).

Table 1 Aberrant cell phenotypes and mitotic progression in cells that constitutively expressed SGOL1-P1

	Fixed cells			*Living cells*
	Micronucleus[a] *frequency (%)*	*Extra centrosome*[a] *frequency (%)*	*Mitotic index frequency (%)*	*Immature metaphase*[b] *frequency (%)*
Parent	4/418 (0.96)	1/266 (0.38)	27/1027 (2.63)	0/174 (0.00)
V1-1	5/441 (1.13)	1/282 (0.35)	36/1130 (3.19)	0/158 (0.00)
P3-2	9/452 (1.99)	5/279 (1.79)	48/1106 (4.34)**,†	6/170 (3.53)*,†
P4-1	16/403 (3.97)**,†	8/247 (3.24)*,†	49/1152 (4.25)**,††	13/159 (8.18)**,††

[a]Refer to Figure 6.
[b]Chromosomal mass, separated without metaphase congression or after congression, too brief to be observed in images acquired at 5-min intervals. Statistical analyses were performed by using the χ^2-test for the mitotic index data and Fisher's exact test for other data.
$^{*}P<0.05$ vs parent, $^{\dagger}P<0.05$ vs V1-1, $^{**}P<0.01$ vs parent and $^{\dagger\dagger}P<0.01$ vs V1-1.

The concept that tumors are composed of a heterogeneous population of cells has been established (Reya *et al*., 2001). Cancer stem cells (CSCs) exhibit both properties of self-renewal and differentiation into diverse cancer cell types and they are thought to be responsible for tumors being composed of a heterogeneous population of cells. When chromosomal abnormalities occur in CSCs, the phenotypic diversity of the cells in a tumor may increase and have a negative impact on the outcome, because of the acquisition of malignant properties, such as drug resistance and metastasis. Therefore, it is also expected that shugoshin studies will be performed in the field of CSCs in order to investigate its impact on tumor progression.

Aberrant chromosome alignment at the metaphase plate is thought to be due to unstable chromatid cohesion. It has

recently been reported that a mono-oriented chromosome is transported toward the metaphase plate along the kinetochore fiber that has already attached to the bi-oriented chromosomes remaining at the metaphase plate (Kapoor *et al.*, 2006), and that cohesion between chromatids at the centromere influences kinetochore geometry and determines kinetochore orientation (Sakuno *et al.*, 2009). Therefore, inappropriate kinetochore orientation is thought to cause the defect in transport to the metaphase plate and result in the aberrant chromosome alignment in cells expressing SGOL1-P1.

The number of cells that contained an extra centrosome increased in the presence of SGOL1-P1 in our experiment. This finding was consistent with the results of a previous study in which spindle pole integrity was found to require chromosome cohesion (Dai *et al.*, 2009). In that study, knockdown of haspin, SGOL1 or RAD21, all of which are necessary for chromosome cohesion, resulted in an increase in the number of γ-tubulin foci. Thus, the overexpression of SGOL1-P1 should also impair centrosome stability by interfering with chromatid cohesion.

This is the first study to report an association between cancer and a SGOL1 variant. As SGOL1-P1 expression inhibited the localization of endogenous SGOL1 and RAD21 to the centromere in our experiments, SGOL1-P1 is thought to function as a negative factor to native SGOL1. Although the details of the molecular mechanism mediated by SGOL1-P1 remain unclear, a protein–protein interaction with an, as yet, unidentified protein is assumed to be involved in the mechanism. SGOL1-P1 is composed of 59 amino acids, and the region of SGOL1-A1 protein (amino acids 1–47) encoded by exon 1 and exon 2 of the *SGOL1* gene accounts for 79.7% of the amino acid sequence of SGOL1-P1. Having the amino acid sequence 51–96 is sufficient for SGOL1 to bind PP2A (Xu *et al.*, 2009). This amino acid region is within the exon 3-coded region (aa 48–113), and SGOL1 mutant N61I actually does not exhibit binding activity to PP2A (Tang *et al.*, 1998, 2006; Xu *et al.*, 2009). Thus, PP2A is probably not a target of SGOL1-P1. Actually, the localization of PP2A-B56α on chromosomes was not affected by SGOL1-P1 expression, even in cells with a reduction in RAD21 signals. Similarly, heterochromatin protein HP1α, a SGOL1-interacting protein that is required for localization and functioning of SGOL1 at the centromere does not seem to be a target either, because the binding region of SGOL1 to HP1α is located in the C-terminal area (Yamagishi *et al.*, 2008). As it is more likely that SGOL1-P1 inhibits the interaction between native SGOL1 and as yet unidentified targets, we are currently searching for proteins that interact with SGOL1-P1.

There is also the possibility that the SGOL1-P1-unique sequence may be involved in abnormal chromosome alignment. The C-terminal short region of SGOL1-P1 corresponds to exon 4 in the frameshift and this frameshift is what makes the SGOL1-P1 sequence unique among SGOL1 variants. Interestingly, a BLAST search of the NCBI's protein database revealed that the C-terminal unique sequence of SGOL1-P1 is similar to the conserved region of the Polo-like kinase (Plk) family. The part of the sequence in the Plk family proteins that is similar to the C-terminal unique sequence of SGOL1-P1 and the adjacent residues are conserved among species and form a catalytic loop (Supplementary Figure S7; Kothe *et al.*, 2007). The results of the NCBI's Conserved Domains Database search also suggested that the Plk1 catalytic loop includes ATP- and substrate-binding sites (accession number cd05123), and thus SGOL1-P1 may interfere with Plk1-mediated phosphorylation through the conserved region described above. If this model, in which SGOL1-P1 targets Plk1, is correct, the abnormal chromosome alignment and the precociously separated chromatids found in the SGOL1-P1-expressing cells should be independent of each other, because Plk1 is required for assembly of the mitotic spindle, but not for chromatid cohesion (Losada *et al.*, 2002; Sumara *et al.*, 2002, 2004; Eot-Houllier *et al.*, 2008). The spatio-temporal function of SGOL1-P1 in relation to Plk1 and native SGOL1 may cause the abnormal mitotic phenotypes observed in the present study.

The results of the present study demonstrated an association between SGOL1-P1 and colon cancer, and they suggest that native SGOL1 is deregulated by SGOL1-P1. Further studies, such as studies of SGOL1-P1 expression in other types of cancer, of the mechanism of generation of SGOL1-P1 transcripts and of the molecular targets of SGOL1-P1, should improve our understanding of how tumors are generated and become malignant.

Materials and methods

RT–PCR and plasmid construction

RT–PCR was carried out as described in our previous report (Iwaizumi *et al.*, 2009). The primer sequences used for the first RT–PCR (Figure 1b) were 5′-GGAGGAGGAAGATAG CTGTTGC-3′ (sense) and 5′-TATGGCAATGGCTCACTC TG-3′ (antisense). The PCR products from non-tumor tissue and tumor tissue were cloned and used for the sequence analysis. A primer targeting the junction between exon 2 and exon 4 was constructed for routine detection of *SGOL1-P1* transcripts in specimens (Supplementary Figure S1). Glyceraldehyde-3-phosphate dehydrogenase (GAPDH) was amplified as an internal control, and the quantitative real-time RT–PCR was carried out as described previously (Iwaizumi *et al.*, 2009). To express SGOL1-P1 in mammalian cells, six myc tags were fused to the N-terminus of SGOL1-P1 and the product was inserted into pcDNA3.1. The pSilencer plasmid with short hairpin RNA (shRNA) targeting the SGOL1 sequence was used for the RNA interference (RNAi) procedure as described previously (Iwaizumi *et al.*, 2009).

Cell culture and transfection

Human colon cancer cell line HCT116 was cultured at 37 °C in RPMI medium (Invitrogen, Carlsbad, CA, USA) containing 10% fetal bovine serum (Nichirei, Tokyo, Japan), under 5% CO_2. Transfection was performed by using Lipofectamine 2000 (Invitrogen) according to the manufacturer's protocol. Stable cell lines expressing myc-SGOL1 (A1 or P1) were generated by incubating the transfected cells in selection medium containing 200 μg/ml geneticin (Invitrogen) and

performing limiting-dilution cloning. Cells subcultured for 25–45 passages were used in the experiments.

Antibodies
Rabbit polyclonal anti-shugosin (ab21633; Abcam, Cambridge, MA, USA; Figure 2c), anti-myc tag (06-549; Millipore, Bedford, MA, USA) and anti-Rad21 antibodies (ab992; Abcam; Figure 4d), mouse polyclonal anti-PPP2R5A antibodies (PP2A-B56α) (H00005525-B01P; Abnova, Taipei, Taiwan) and mouse monoclonal anti-β-tubulin (2-28-33; Sigma, St Louis, MO, USA), anti-hSgo1 (Figure 4b), and anti-Rad21 (53A303; Millipore; Figure 4c) and anti-γ-tubulin antibodies (GTU88; Sigma) were used for immunoblotting and immunofluorescence staining. Human autoantibody against the centromere (Immunovison, Springdale, AR, USA) was used for immunofluorescence staining of kinetochore. HRP-conjugated donkey polyclonal anti-rabbit antibody or anti-mouse IgG antibody (GE Healthcare, Piscataway, NJ, USA) and Alexa Fluor 488/546/633-conjugated goat polyclonal anti-rabbit, anti-mouse or anti-human IgG antibodies (Invitrogen) were used as secondary antibodies.

Immunoblotting
Immunoblotting was performed as described previously (Kahyo *et al*., 2008). Briefly, the protein concentration of the lysate was measured with a BCA protein assay kit (Thermo Scientific, Rockford, IL, USA). Following the addition of SDS sample buffer, the samples were boiled at 95 °C for 5 min and they were then subjected to SDS–polyacrylamide gel electrophoresis. Cell lysate of 10 μg was loaded on the gel.

Confocal laser scanning
Cells plated on fibronectin-coated glass coverslips (Becton Dickinson, Franklin Lakes, NJ, USA) were transfected with myc-SGOL1 or shRNA of SGOL1 and cultured for 24 h. The cells were cultured in presence of puromycin (0.8 μg/ml, Sigma) for RNAi or geneticin (200 μg/ml) for the expression assay. After culture for 48 h, they were fixed with 4% paraformaldehyde in phosphate-buffered saline (PBS) buffer (140 mM NaCl, 2.7 mM KCl, 8.1 mM sodium phosphate dibasic and 1.5 mM potassium phosphate monobasic) at room temperature for 15 min, permealized with 0.1% Triton X-100 and subjected to immunostaining. For γ-tubulin, staining cells were fixed with cold methanol at −20 °C for 5 min. To detect RAD21 and PP2A-B56α signals on the chromosomes clearly, we referred to previous reports (Waizenegger *et al*., 2000; Kitajima *et al*., 2006; Lee *et al*., 2008). Briefly, cultured cells were spun on a glass coverslip for 5 min at 290 *g* and pre-treated with 0.1% Triton X-100 in PBS at room temperature for 2 min before fixation with 4% paraformaldehyde. All of the cells were stained with 1.5 μg/ml 4′,6-diamidine-2-phenylindole (DAPI, Invitrogen) to visualize their nuclei. Fluorescence signals were detected by confocal laser scanning microscopy (FV1000; Olympus, Tokyo, Japan). The lengths of horizontal and vertical axes were measured with Image J software (version 1.43f; National Institutes of Health, Bethesda, MD, USA).

Chromosome spread
Transfected cells were selected with antibiotics as described above. After culture for 48 h, the cells were treated with 100 nM nocodazole (Sigma) for 18 h. They were then trypsinized and collected by centrifugation in a conical tube. The cells were gently suspended with hypotonic solution (75 mM KCl) and incubated at 37 °C for 6 min. Chilled fixative solution (methanol:glacial acetic acid, 3:1) was gently added to the cells that had been collected by centrifugation, and this procedure consisting of centrifugation, collection of the cells and addition of chilled fixative solution was repeated three times. The fixed cells were dropped onto the slide glasses. After drying in air, they were stained with DAPI.

Time-lapse imaging
Myc-SGOL1 and GFP-Histone H2B plasmids were used to co-transfect HCT116 cells plated on the fibronectin-coated glass-bottom dishes, and 48 h later, the medium was replaced with fresh medium and the cells were subjected to time-lapse imaging (FCV100; Olympus). Fluorescence signals from GFP were captured at 5 min intervals for 24 h and the data were used to prepare the montage images and movies.

Statistical analysis
The Mann–Whitney *U*-test was used to statistically analyze non-parametric data. The χ^2-test or Fisher's exact test was used to compare categorical variables. The statistical analysis was performed by using the Microsoft Excel software program (Microsoft, Redman, WA, USA).

Ethics
The design of this study, including the human genomics and recombinant DNA research, was approved by the Institutional Review Board of Hamamatsu University School of Medicine.

Conflict of interest

The authors declare no conflict of interest.

Acknowledgements

We thank Dr Suzuki of The Jikei University School of Medicine for providing the anti-hSgo1 antibody. This work was supported by a Grant-in-Aid for Scientific Research (C) (22590356) and for priority areas (20014007 and 221S0001) from the Japanese Ministry of Education, Culture, Sports, Science and Technology, Grants-in-Aid for the 3rd Term Comprehensive 10-Year-Strategy for Cancer Control and Grants-in-Aid for Cancer Research from the Japanese Ministry of Health (21-1) and from the Smoking Research Foundation.

References

Bharadwaj R, Yu H. (2004). The spindle checkpoint, aneuploidy, and cancer. *Oncogene* **23**: 2016–2027.

Clift D, Bizzari F, Marston AL. (2009). Shugoshin prevents cohesin cleavage by PP2A(Cdc55)-dependent inhibition of separase. *Genes Dev* **23**: 766–780.

Dai J, Kateneva AV, Higgins JM. (2009). Studies of haspin-depleted cells reveal that spindle-pole integrity in mitosis requires chromosome cohesion. *J Cell Sci* **122**: 4168–4176.

Eot-Houllier G, Fulcrand G, Watanabe Y, Magnaghi-Jaulin L, Jaulin C. (2008). Histone deacetylase 3 is required for centromeric

H3K4 deacetylation and sister chromatid cohesion. *Genes Dev* **22**: 2639–2644.

Gisselsson D, Bjork J, Hoglund M, Mertens F, Dal Cin P, Akerman M *et al.* (2001). Abnormal nuclear shape in solid tumors reflects mitotic instability. *Am J Pathol* **158**: 199–206.

Goldstein LS. (1980). Mechanisms of chromosome orientation revealed by two meiotic mutants in Drosophila melanogaster. *Chromosoma* **78**: 79–111.

Grady WM. (2004). Genomic instability and colon cancer. *Cancer Metastasis Rev* **23**: 11–27.

Hauf S, Waizenegger IC, Peters JM. (2001). Cohesin cleavage by separase required for anaphase and cytokinesis in human cells. *Science* **293**: 1320–1323.

Iwaizumi M, Shinmura K, Mori H, Yamada H, Suzuki M, Kitayama Y *et al.* (2009). Human Sgo1 downregulation leads to chromosomal instability in colorectal cancer. *Gut* **58**: 249–260.

Kahyo T, Mostoslavsky R, Goto M, Setou M. (2008). Sirtuin-mediated deacetylation pathway stabilizes Werner syndrome protein. *FEBS Lett* **582**: 2479–2483.

Kanda T, Sullivan KF, Wahl GM. (1998). Histone-GFP fusion protein enables sensitive analysis of chromosome dynamics in living mammalian cells. *Curr Biol* **8**: 377–385.

Kapoor TM, Lampson MA, Hergert P, Cameron L, Cimini D, Salmon ED *et al.* (2006). Chromosomes can congress to the metaphase plate before biorientation. *Science* **311**: 388–391.

Karamysheva Z, Diaz-Martinez LA, Crow SE, Li B, Yu H. (2009). Multiple anaphase-promoting complex/cyclosome degrons mediate the degradation of human Sgo1. *J Biol Chem* **284**: 1772–1780.

Kawashima SA, Yamagishi Y, Honda T, Ishiguro K, Watanabe Y. (2010). Phosphorylation of H2A by Bub1 prevents chromosomal instability through localizing shugoshin. *Science* **327**: 172–177.

Kerrebrock AW, Moore DP, Wu JS, Orr-Weaver TL. (1995). Mei-S332, a Drosophila protein required for sister-chromatid cohesion, can localize to meiotic centromere regions. *Cell* **83**: 247–256.

Kienitz A, Vogel C, Morales I, Muller R, Bastians H. (2005). Partial downregulation of MAD1 causes spindle checkpoint inactivation and aneuploidy, but does not confer resistance towards taxol. *Oncogene* **24**: 4301–4310.

Kitajima TS, Hauf S, Ohsugi M, Yamamoto T, Watanabe Y. (2005). Human Bub1 defines the persistent cohesion site along the mitotic chromosome by affecting Shugoshin localization. *Curr Biol* **15**: 353–359.

Kitajima TS, Kawashima SA, Watanabe Y. (2004). The conserved kinetochore protein shugoshin protects centromeric cohesion during meiosis. *Nature* **427**: 510–517.

Kitajima TS, Sakuno T, Ishiguro K, Iemura S, Natsume T, Kawashima SA *et al.* (2006). Shugoshin collaborates with protein phosphatase 2A to protect cohesin. *Nature* **441**: 46–52.

Kothe M, Kohls D, Low S, Coli R, Cheng AC, Jacques SL *et al.* (2007). Structure of the catalytic domain of human polo-like kinase 1. *Biochemistry* **46**: 5960–5971.

Lee J, Kitajima TS, Tanno Y, Yoshida K, Morita T, Miyano T *et al.* (2008). Unified mode of centromeric protection by shugoshin in mammalian oocytes and somatic cells. *Nat Cell Biol* **10**: 42–52.

Lengauer C, Kinzler KW, Vogelstein B. (1998). Genetic instabilities in human cancers. *Nature* **396**: 643–649.

Losada A, Hirano M, Hirano T. (2002). Cohesin release is required for sister chromatid resolution, but not for condensin-mediated compaction, at the onset of mitosis. *Genes Dev* **16**: 3004–3016.

Lupas A, Van Dyke M, Stock J. (1991). Predicting coiled coils from protein sequences. *Science* **252**: 1162–1164.

Marston AL, Tham WH, Shah H, Amon A. (2004). A genome-wide screen identifies genes required for centromeric cohesion. *Science* **303**: 1367–1370.

Mayr C, Bartel DP. (2009). Widespread shortening of 3′UTRs by alternative cleavage and polyadenylation activates oncogenes in cancer cells. *Cell* **138**: 673–684.

McGuinness BE, Hirota T, Kudo NR, Peters JM, Nasmyth K. (2005). Shugoshin prevents dissociation of cohesin from centromeres during mitosis in vertebrate cells. *PLoS Biol* **3**: e86.

Moore DP, Page AW, Tang TT, Kerrebrock AW, Orr-Weaver TL. (1998). The cohesion protein MEI-S332 localizes to condensed meiotic and mitotic centromeres until sister chromatids separate. *J Cell Biol* **140**: 1003–1012.

Nasmyth K, Peters JM, Uhlmann F. (2000). Splitting the chromosome: cutting the ties that bind sister chromatids. *Science* **288**: 1379–1385.

Peters JM. (2002). The anaphase-promoting complex: proteolysis in mitosis and beyond. *Mol Cell* **9**: 931–943.

Pihan GA, Doxsey SJ. (1999). The mitotic machinery as a source of genetic instability in cancer. *Semin Cancer Biol* **9**: 289–302.

Rabitsch KP, Gregan J, Schleiffer A, Javerzat JP, Eisenhaber F, Nasmyth K. (2004). Two fission yeast homologs of Drosophila Mei-S332 are required for chromosome segregation during meiosis I and II. *Curr Biol* **14**: 287–301.

Rajagopalan H, Lengauer C. (2004). Aneuploidy and cancer. *Nature* **432**: 338–341.

Reya T, Morrison SJ, Clarke MF, Weissman IL. (2001). Stem cells, cancer, and cancer stem cells. *Nature* **414**: 105–111.

Riedel CG, Katis VL, Katou Y, Mori S, Itoh T, Helmhart W *et al.* (2006). Protein phosphatase 2A protects centromeric sister chromatid cohesion during meiosis I. *Nature* **441**: 53–61.

Sakuno T, Tada K, Watanabe Y. (2009). Kinetochore geometry defined by cohesion within the centromere. *Nature* **458**: 852–858.

Salic A, Waters JC, Mitchison TJ. (2004). Vertebrate shugoshin links sister centromere cohesion and kinetochore microtubule stability in mitosis. *Cell* **118**: 567–578.

Shinmura K, Iwaizumi M, Igarashi H, Nagura K, Yamada H, Suzuki M *et al.* (2008). Induction of centrosome amplification and chromosome instability in p53-deficient lung cancer cells exposed to benzo[a]pyrene diol epoxide (B[a]PDE). *J Pathol* **216**: 365–374.

Sumara I, Gimenez-Abian JF, Gerlich D, Hirota T, Kraft C, de la Torre C *et al.* (2004). Roles of polo-like kinase 1 in the assembly of functional mitotic spindles. *Curr Biol* **14**: 1712–1722.

Sumara I, Vorlaufer E, Stukenberg PT, Kelm O, Redemann N, Nigg EA *et al.* (2002). The dissociation of cohesin from chromosomes in prophase is regulated by Polo-like kinase. *Mol Cell* **9**: 515–525.

Suzuki H, Akiyama N, Tsuji M, Ohashi T, Saito S, Eto Y. (2006). Human Shugoshin mediates kinetochore-driven formation of kinetochore microtubules. *Cell Cycle* **5**: 1094–1101.

Tang TT, Bickel SE, Young LM, Orr-Weaver TL. (1998). Maintenance of sister-chromatid cohesion at the centromere by the Drosophila MEI-S332 protein. *Genes Dev* **12**: 3843–3856.

Tang Z, Shu H, Qi W, Mahmood NA, Mumby MC, Yu H. (2006). PP2A is required for centromeric localization of Sgo1 and proper chromosome segregation. *Dev Cell* **10**: 575–585.

Tang Z, Sun Y, Harley SE, Zou H, Yu H. (2004). Human Bub1 protects centromeric sister-chromatid cohesion through Shugoshin during mitosis. *Proc Natl Acad Sci USA* **101**: 18012–18017.

Waizenegger IC, Hauf S, Meinke A, Peters JM. (2000). Two distinct pathways remove mammalian cohesin from chromosome arms in prophase and from centromeres in anaphase. *Cell* **103**: 399–410.

Wasch R, Robbins JA, Cross FR. (2010). The emerging role of APC/CCdh1 in controlling differentiation, genomic stability and tumor suppression. *Oncogene* **29**: 1–10.

Xu Z, Cetin B, Anger M, Cho US, Helmhart W, Nasmyth K *et al.* (2009). Structure and function of the PP2A-shugoshin interaction. *Mol Cell* **35**: 426–441.

Yamagishi Y, Sakuno T, Shimura M, Watanabe Y. (2008). Heterochromatin links to centromeric protection by recruiting shugoshin. *Nature* **455**: 251–255.

Supplementary Information accompanies the paper on the Oncogene website (http://www.nature.com/onc)